PHILOSOPHICAL TRANSACTIONS OF THE ROYAL SOCIETY A MATHEMATICAL, PHYSICAL & ENGINEERING SCIENCES

The Diffraction of Two-Dimensional Sound Pulses Incident on an Infinite Uniform Slit in a Perfectly Reflecting Screen

E. N. Fox

Phil. Trans. R. Soc. Lond. A 1949 **242**, 1-32
doi: 10.1098/rsta.1949.0003

THE DIFFRACTION OF TWO-DIMENSIONAL SOUND PULSES INCIDENT ON AN INFINITE UNIFORM SLIT IN A PERFECTLY REFLECTING SCREEN

By E. N. FOX, Ph.D., *Engineering Department, University of Cambridge*

(*Communicated by Sir Geoffrey Taylor, F.R.S.—Received 27 August* 1948)

CONTENTS

In a previous paper (Fox 1948), the general solutions were obtained for the diffraction problems of a perfectly reflecting infinite strip or half-plane subjected to any incident pulse field in two dimensions. A general method is now outlined by which the results of this previous paper could be used without *formal* difficulty to derive solutions for any two-dimensional diffraction problem involving strips and/or half-planes as obstacles. This method is applied to the problem of a perfectly reflecting plane screen containing an infinite slit of uniform width subjected to any known incident pulse field.

The special case of a plane sharp-fronted pulse of constant unit pressure incident normally on such a screen is examined numerically. The most interesting pressure phenomena to the rear of the screen are those occurring in the direct line of the slit where the pressure front exhibits an initial peak which becomes progressively thinner as the front travels farther to the rear. Apart from this effect, the general process of ultimate pressure equalization through the slit appears to be of an asymptotic character, there being no evidence that the pressure at any point to the rear ever exceeds the incident unit pressure. The results also indicate that a region of sensibly incompressible flow is soon developed in the neighbourhood of the slit, this region increasing in size with increasing time. Finally, it is found that the slit behaves, to fair accuracy, as a central two-dimensional source relatively soon after the arrival of the pressure front, for all points to the rear more distant than about $5a$ from the centre of the slit, where $2a$ is the width of the slit. This result and the preceding incompressible flow phenomenon enable approximate solutions to be obtained for particular use at later times when the calculation of the exact solution involving separate diffraction waves becomes unmanageable.

Vol. 242. A. 839. (Price 7*s*. 6*d*.) 1 [Published 25 May 1949

1. Introduction

In a previous paper (Fox 1948) the author has given the solution for an infinite perfectly reflecting strip subjected to any two-dimensional field of sound pulses. For brevity, this previous paper will be referred to as paper I, and its equations will be quoted with a prefix I to distinguish them from the equations of the present paper.

The related two-dimensional problem involving an infinite uniform slit in a perfectly reflecting screen will be considered in the present paper with particular reference to the case of a plane pulse of $H(t)$ shape arriving at normal incidence.

Both the slit and the strip are special cases of a plane screen with apertures for which it was shown in paper I that the complete pressure field can be explicitly obtained if either (a) the pressure gradient through the apertures or (b) the pressure on the back of the screen can be obtained. These latter can in fact be derived for the slit by following the same method as in paper I, namely, the derivation of an integral equation which, when transformed by the Laplace transformation, can be solved by using the basic relation I (52) to give a final series solution corresponding to successive diffraction waves. Nothing essentially new in the mathematics arises, however, in such further application of the integral equation method, and it has been thought more instructive to use an alternative approach of a more physical character in the present paper. This physical approach uses the final results of paper I and serves in particular to illustrate how more complicated problems involving strips as obstacles could theoretically be tackled. We start therefore by considering the general basis of such a method and then proceed to the specific problem of the slit.

2. General method of solution

In paper I, the incident field of pressure on an obstacle such as a screen was defined simply as the pressure in the absence of the obstacle. This definition will now be generalized for several obstacles so that scattered waves from one obstacle can be treated as part of the incident field on a second obstacle.

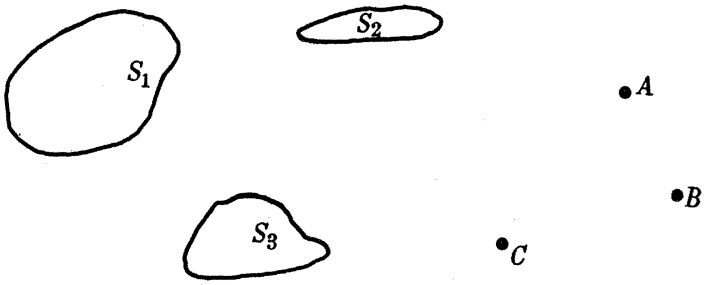

Figure 1.

Consider the general case of pulses originating from any combination of sources $A, B, C, \ldots$ in three dimensions and impinging on any arbitrary arrangement of obstacles $S_1, S_2, \ldots, S_k$, as illustrated in two dimensions by figure 1.

In the absence of *all* obstacles let the total pressure at any point (x, y, z) due to all the sources be $p_i(t, x, y, z)$ which will be termed the *external* pulse field. Let the corresponding pressure at (x, y, z) with all obstacles present be $p(t, x, y, z)$.

Now apply Kirchhoff's solution of the wave equation (Jeans 1925, p. 522) to the medium bounded externally by a sphere of large radius R and internally by the surfaces $S_1, S_2, \ldots, S_k$ and small spheres of radius ϵ round the sources $A, B, C, \ldots$. By taking R large enough we can enclose all sources and all obstacles and, moreover, we can ensure that for any finite time t the large sphere gives zero contribution to Kirchhoff's solution. Similarly, by letting $\epsilon \to 0$, the total contribution of the small spheres round the sources will be simply the pressure in the absence of the obstacles, namely, $p_i(t, x, y, z)$.

Kirchhoff's solution can therefore be written in the form

$$p(t,x,y,z) = p_i(t,x,y,z) - \frac{1}{4\pi}\sum_{q=1}^{k}\iint\left[\frac{1}{cr}\frac{\partial r}{\partial n}\frac{\partial p}{\partial t} - p\frac{\partial}{\partial n}\left(\frac{1}{r}\right) + \frac{1}{r}\frac{\partial p}{\partial n}\right]_{t-r/c} dS_q, \tag{1}$$

where the integrals are taken over the surfaces of the different obstacles, c is the velocity of sound, r is the distance from (x, y, z) to any point on the surface S_q of outward normal n into the medium, and the integrand is to be evaluated at time $t - r/c$.

The *effective* incident field $p_{im}(t, x, y, z)$ for any one of the obstacles S_m will now be defined by the equation

$$p(t,x,y,z) = p_{im}(t,x,y,z) - \frac{1}{4\pi}\iint\left[\frac{1}{cr}\frac{\partial r}{\partial n}\frac{\partial p}{\partial t} - p\frac{\partial}{\partial n}\left(\frac{1}{r}\right) + \frac{1}{r}\frac{\partial p}{\partial n}\right]_{t-r/c} dS_m, \tag{2}$$

in which the surface integral is taken over S_m only.

Comparing (1) and (2) we see that p_{im} includes all contributions to the pressure p except the term in the Kirchhoff solution arising from S_m itself. As thus defined, the effective incident field differs for each of the obstacles; but this is not unreasonable on the physical basis that each external pulse produces scattered waves when it strikes any obstacle, and these scattered waves are then in turn incident, in general, on the other obstacles.

When there is only one obstacle S_1, the effective incident field $p_{i1} = p_i$, the pressure in the absence of the obstacle, and the present definition is then equivalent to the definition of incident field given in paper I.

If desired, any group of obstacles $S_1, \ldots, S_j$ can be treated as a single obstacle by defining their incident field as the contribution in equation (1) of $p_i(t, x, y, z)$ and the integrals over the remaining obstacles $S_{j+1}, \ldots, S_k$. In this way a regular grating, for example, can be considered as a single obstacle, and if no other obstacles are present the effective incident field is simply the external pulse field p_i; alternatively, each strip can be treated as a separate obstacle subjected to an effective incident field which includes scattered waves from the other strips.

Returning to the general problem, the *scattered* field p_m originating from the surface S_m is defined by

$$p_m(t,x,y,z) = -\frac{1}{4\pi}\iint\left[\frac{1}{cr}\frac{\partial r}{\partial n}\frac{\partial p}{\partial t} - p\frac{\partial}{\partial n}\left(\frac{1}{r}\right) + \frac{1}{r}\frac{\partial p}{\partial n}\right]_{t-r/c} dS_m, \tag{3}$$

and equation (3) may then be written

$$p = p_{im} + p_m, \tag{4}$$

where from (1) and (3)

$$p_{im} = p_i + \sum_{q=1}^{m-1} p_q + \sum_{q=m+1}^{k} p_q. \tag{5}$$

Equation (4) gives k different ways of subdividing the total field, and a problem involving k obstacles can correspondingly be considered as k separate problems each involving one obstacle only.

For perfectly reflecting surfaces $\partial p/\partial n = 0$, and if the problem for each obstacle can separately be solved to give the pressure on the obstacle in terms of the effective incident field p_{im}, a series of k simultaneous equations would be obtained relating the pressure distributions on each obstacle and the external incident field p_i.

Provided all obstacles are a finite distance apart there is then no formal difficulty, as illustrated later for the slit problem, in solving these equations in successive stages corresponding to the finite intervals of time involved in the successive interaction of the scattered fields. In particular, as concluded in paper I, the solution for the strip problem implies no formal difficulties in solving any arbitrary arrangement of separate strips subjected to two-dimensional pulses; the labour of numerical evaluation would, however, undoubtedly be prohibitive in all but relatively simple cases.

Consider now, as in paper I, the case where the obstacle S_m is a perfectly reflecting plane screen with apertures. The surface integral in (2) and (3) is then taken over *both* sides of the screen excluding the apertures; this is in contrast to the corresponding discussion of paper I where Kirchhoff's solution was applied to the rear only of the screen including the apertures.

For complete reflexion $\partial p/\partial n = 0$ and equation (3) becomes

$$p_m(t,x,y,z) = -\frac{1}{4\pi}\iint\left[\frac{1}{cr}\frac{\partial r}{\partial n}\frac{\partial p}{\partial t} - p\frac{\partial}{\partial n}\left(\frac{1}{r}\right)\right]_{t-r/c} dS_m. \tag{6}$$

Taking the plane of the screen as $x = 0$, we obtain similarly for the image point $(-x,y,z)$

$$p_m(t,-x,y,z) = -\frac{1}{4\pi}\iint\left[\frac{1}{cr'}\frac{\partial r'}{\partial n}\frac{\partial p}{\partial t} - p\frac{\partial}{\partial n}\left(\frac{1}{r'}\right)\right]_{t-r'/c} dS_m. \tag{7}$$

But, as in equation I (6), the distances r, r' of the points (x,y,z), $(-x,y,z)$ from any element dS_m on either face of the screen are related by

$$r' = r, \quad \frac{\partial r'}{\partial n} = -\frac{\partial r}{\partial n}. \tag{8}$$

Hence from (6), (7) and (8) we have

$$p_m(t,x,y,z) = -p_m(t,-x,y,z). \tag{9}$$

Thus the scattered field due to any plane reflecting obstacle gives equal and opposite pressure contributions at image points. For the special case of a point $(0,y,z)$ in an aperture of the screen

$$\frac{\partial r}{\partial n} = 0$$

for every element dS_m; hence from (6)

$$p_m(t,0,y,z) = 0 \tag{10}$$

for any point in an aperture. This corresponds to equation (9) with continuity of pressure p_m across the aperture. A similar result does not, of course, hold for a point on the reflecting surface of the screen since $r \to 0$ for elements surrounding the point, and it is necessary to

consider the limiting case when $\epsilon \to 0$ of pressure at a point distant ϵ from the screen. If this limiting process is applied to either (6) or (7), representing points on either side, the result is simply equation (9) with $x = 0$. For such points the pressure will in general be different on the two faces of the screen.

If we now apply equation (4) to image points in turn and add the resulting equations, in view of (9), we obtain

$$p(t, x, y, z) + p(t, -x, y, z) = p_{im}(t, x, y, z) + p_{im}(t, -x, y, z). \tag{11}$$

Similarly, from (4) and (10), we obtain

$$p = p_{im} \tag{12}$$

for any point $(0, y, z)$ in an aperture. As thus deduced, it may be noted that (12) does not depend on assuming continuity of the pressures p and p_{im} across the aperture which does not necessarily hold when a further obstacle occupies part of the aperture; this point is illustrated in the solution given later for the slit problem regarded as two separate half-planes, each of which then occupies part of the aperture relevant to the other.

At a point on the reflecting part of the screen, provided no other obstacle is in contact with it, the effective incident pressure p_{im} will in general be continuous and equation (11) leads to

$$p_f + p_b = 2p_{im}, \tag{13}$$

where the suffixes f and b refer to the front and back of the screen.

Equations (11), (12) and (13) differ only from the basic equations I (1), I (2) and I (3) of the previous paper, in that p_{im} replaces p_i. This indicates, as we should expect physically, that the results of paper I can be used not only for pulses arriving from external sources but also for the scattered fields from other obstacles arriving at a strip or half-plane.

From the physical standpoint it is convenient to think of the scattered field originating from any strip or half-plane as being composed of constituent waves. Consider, for example, the simple case of paper I in which a strip is subjected to a plane pulse arriving at normal incidence. In this case, the total pressure field at any point consists in effect of contributions from (*a*) the diffraction waves sent out from either edge into all regions, (*b*) the incident plane pulse in all regions except the shadow and (*c*) a reflected pulse existing only in the region directly in front of the strip. To obtain the scattered field as previously defined we must subtract the incident pulse in *all* regions to leave (*a*) the diffraction waves from the two edges contributing in all regions, (*b*) the reflected pulse in the region immediately in front of the strip and (*c*) a 'cut-off' wave propagated to the rear in the shadow and exactly cancelling the incident pulse in this region. It is easy to overlook this third constituent, since it only manifests itself indirectly as the absence of the incident pulse. Strictly, all these constituent waves form a single entity corresponding to the total disturbance produced by the strip. In particular, at the boundaries of either the shadow or the reflexion region the cut-off or reflected wave respectively ceases to exist, and the resulting discontinuities are balanced by corresponding discontinuities in the relevant diffraction waves. As illustrated later in the solution for the slit problem it is essential to bear in mind this point that a diffraction wave is not in general a separate entity but only exists in conjunction with reflected and 'cut-off' waves.

A similar physical interpretation can be made in the general case of a plane screen with apertures. Thus, for any incident field p_{im} arriving from sources or obstacles on one side of the screen, the scattered field p_m can be regarded as consisting of (i) reflected waves in partial regions to the front, (ii) cut-off waves in the image shadow regions to the rear, and (iii) diffraction waves from the edges of the apertures sent out into all regions. For perfect reflexion, the reflected and 'cut-off' waves will give equal and opposite contributions at any point and its image point respectively, and, since the total scattered field is also equal and opposite at such points by (9), it follows that the pressure in diffraction waves will likewise be of equal magnitude but opposite sign at image points in the screen.

3. Slit in perfectly reflecting screen subjected to any two-dimensional pulse field

Consider the problem of figure 2 in which a slit BC of uniform width $2a$ formed by two coplanar perfectly reflecting half-planes AB and CD is subjected to an external two-dimensional pulse field $p_i(t, x, y)$.

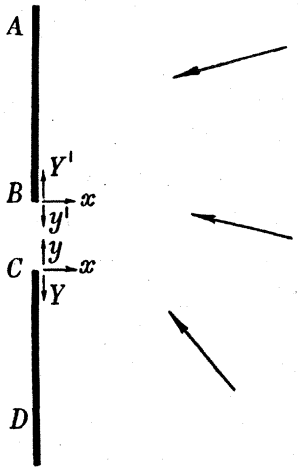

Figure 2

Without loss of generality we can assume the external pulses to be arriving from the right $x > 0$, since the problem for pulses arriving from the left is essentially the same, and we can superpose to obtain the solution for pulses coming from both directions. Since the two half-planes in combination can be considered as a single obstacle of the form of a plane screen with one aperture, we can use equations I (1) and I (7) or I (9) to give the complete solution, provided we can obtain either (*a*) the distribution of the pressure gradient

$$-\frac{\partial p}{\partial n} = \frac{\partial p}{\partial x} = \psi(y, t) \quad (x = 0), \tag{14}$$

over the slit or (*b*) the distribution of the pressure p_b on the back of the half-planes which we shall denote by

$$\left.\begin{aligned} p_b &= F(Y, t) \quad \text{on rear of } CD \text{ (figure 2)},\\ p_b &= F(Y', t) \quad \text{on rear of } AB \text{ (figure 2)}. \end{aligned}\right\} \tag{15}$$

These basic solutions we shall derive by considering each half-plane as a separate obstacle and using the general solution for a half-plane given in appendix B of paper I.

We make the problem non-dimensional by taking the width $2a$ of the slit as our unit of length and the time $2a/c$ for a sound wave to travel this width as our unit of time; in these units the wave velocity is unity. The plane $ABCD$ is taken as $x = 0$, and it is convenient to introduce the four symbols y, Y, y', Y' to denote positive distances measured from either edge of the slit as shown in figure 2; these distances are then connected by the relations

$$y = -Y = 1 + Y' = 1 - y'. \tag{16}$$

It is further convenient, in order to use the inherent symmetry of the slit, to use the dual notation

$$p_i(y, t) \equiv p_i'(y', t) \tag{17}$$

to denote values of the external incident pressure when $x = 0$, regarded as functions of t and y or y' respectively.

Regarding each half-plane as a separate obstacle we can write the general equation (1) in the form

$$p(t, x, y) = p_i(t, x, y) + p_1(t, x, y) + p_2(t, x, y), \tag{18}$$

where p_1 and p_2 refer to the scattered fields from the lower and upper half-plane respectively.

The effective incident field for the lower half-plane is then

$$p_{i1}(t, x, y) = p_i(t, x, y) + p_2(t, x, y), \tag{19}$$

whilst that for the upper half-plane is

$$p_{i2}(t, x, y) = p_i(t, x, y) + p_1(t, x, y). \tag{20}$$

3·1. *Solution for pressure on the back of the screen*

Consider first the problem of the lower half-plane CD subjected to an incident field p_{i1} defined by (19). The relevant solution is equation I (161) of paper I, which gives the pressure on the rear of the half-plane in terms of the incident pressure at points above it in the same plane. In the present problem the term p_2 in the effective incident field p_{i1} has different values on opposite sides of the upper half-plane, and there is an apparent ambiguity. This is most easily resolved by considering the actual problem as the limiting case of one in which the upper half-plane is displaced a small distance $\epsilon \to 0$ to the right of the plane $x = 0$ of the lower half-plane. The value of p_2 to be used in the solution is then clearly the value on the rear of the upper half-plane. Consideration of the other limiting process in which the upper plane is displaced to the left would, of course, lead ultimately to the same solution but is more complicated, since the scattered field p_2 would then arrive from the left whereas p_i arrives from the right.

The relevant values of p_{i1}, to be inserted in equation I (161) in place of p_i, are thus the values in the aperture BC and on the rear of AB (figure 2). But by (10) we have $p_1 = p_2 = 0$ on BC, whence

$$p_{i1} = p_i(y, t) \quad (x = 0,\ 0 \leqslant y \leqslant 1), \tag{21}$$

whilst on the rear of AB we have $p_1 = 0$ and from (18), (19) and (15)

$$p_{i1} = F(Y', t) = p_i(y, t) + \{F(Y', t) - p_i(y, t)\} \quad (x = 0,\ 1 \leqslant y = 1 + Y'). \tag{22}$$

Hence, applying I (161), with p_{i1} for p_i, to the problem for the lower half-plane, the solution for the pressure on the back can be written in the form

$$F(Y,t) = \frac{1}{\pi}\int_0^\infty \frac{p_i(y, t-y-Y)}{y+Y}\sqrt{\left(\frac{Y}{y}\right)}\,dy + \frac{1}{\pi}\int_0^\infty \frac{\{F'(Y', t-1-Y'-Y) - p_i(Y'+1, t-1-Y'-Y)\}}{1+Y+Y'}\sqrt{\left(\frac{Y}{1+Y'}\right)}\,dY' \quad (Y>0). \tag{23}$$

In this form, the first term represents the direct effect of the external incident field, and the second term gives the effect of the scattered field from the upper half-plane.

Similarly, we may consider the separate problem of the upper half-plane subjected to an effective incident field p_{i2}, and a second equation will be obtained which, by virtue of the notation we have chosen, is given simply by changing accented to unaccented symbols and conversely, in equation (23). Thus we have also

$$F'(Y',t) = \frac{1}{\pi}\int_0^\infty \frac{p_i'(y', t-y'-Y')}{y'+Y'}\sqrt{\left(\frac{Y'}{y'}\right)}\,dy' + \frac{1}{\pi}\int_0^\infty \frac{\{F(Y, t-1-Y'-Y) - p_i'(Y+1, t-1-Y'-Y)\}}{1+Y+Y'}\sqrt{\left(\frac{Y'}{1+Y}\right)}\,dY \quad (Y'>0). \tag{24}$$

It will be noted in the two equations (23) and (24) that the function F or F' on the left-hand side at time t depends only on values of the other function F' or F for times $t-1$ or earlier. It is thus easy to obtain a solution in the form of successive diffraction waves by assuming series of the type

$$F(Y,t) = F_0(Y,t) + F_1(Y,t) + \ldots + F_r(Y,t) + \ldots, \tag{25}$$

$$F'(Y',t) = F_0'(Y',t) + F_1'(Y',t) + \ldots + F_r'(Y',t) + \ldots. \tag{26}$$

Equation (23) will then be satisfied if

$$F_0(Y,t) = \frac{1}{\pi}\int_0^\infty \frac{p_i(y, t-y-Y)}{y+Y}\sqrt{\left(\frac{Y}{y}\right)}\,dy, \tag{27}$$

$$F_1(Y,t) = \frac{1}{\pi}\int_0^\infty \frac{F_0'(Y', t-1-Y'-Y) - p_i(Y'+1, t-1-Y'-Y)}{1+Y+Y'}\sqrt{\left(\frac{Y}{1+Y'}\right)}\,dY', \tag{28}$$

$$F_{r+1}(Y,t) = \frac{1}{\pi}\int_0^\infty \frac{F_r'(Y', t-1-Y'-Y)}{1+Y+Y'}\sqrt{\left(\frac{Y}{1+Y'}\right)}\,dY' \quad (r\geqslant 1), \tag{29}$$

whilst to satisfy equation (24) we have an exactly similar set of equations with accented changed to unaccented symbols and conversely. The complete six equations thus enable the terms in the series (25) and (26) to be successively determined, and a formal explicit solution for the pressure on the rear of the half-planes is then given by (15), (25) and (26). If the external incident field is symmetrical about the slit the functions F and F' are the same, and we can drop the accents to F_0' and F_r' (but not to Y') in equations (28) and (29). In this case, if the external field p_i first arrives at the edges of the slit at time $t = 0$, then physically we must have

$$p_i(y,t) = 0 \quad (t+y<0), \tag{30}$$

PHILOSOPHICAL TRANSACTIONS OF THE ROYAL SOCIETY A MATHEMATICAL, PHYSICAL & ENGINEERING SCIENCES

and it follows from equation (27) that

$$F_0(Y,t) = 0 \quad (t<Y). \tag{31}$$

Hence by induction it is easy to show from (28) and (29) that, as in the corresponding strip problem of paper I,

$$F_r(Y,t) = 0 \quad (t<r+Y). \tag{32}$$

Conversely, as in paper I for the strip problem, it is easy to show that the solution is the unique solution satisfying the necessary physical condition

$$F(Y,t) = 0 \quad (t<Y), \tag{33}$$

corresponding to no effect being propagated down the rear of a half-plane faster than the unit velocity of sound.

For an unsymmetrical incident field similar relations to (31) and (32) can be obtained, the main feature being that the r-even F_r and r-odd F'_r functions form one set propagated at successive unit intervals of time after the arrival of p_i at the lower edge, whilst the r-even F'_r and r-odd F_r functions form a similar set with time measured from the arrival of p_i at the upper edge. Having obtained the solution for p_b, equations I (9) and I (1) then give the formal explicit solution for the pressure everywhere.

The solution for p_b corresponds to the physical process of the external incident field producing diffraction waves F_0, F'_0 at the two edges which are then each incident on the further edge to produce F'_1, F_1 respectively and so on. An alternative method of solution could be based on this process, *ab initio*, by assuming the forms (25) and (26), where F_0, F'_0 are the solutions for each half-plane in the absence of the other and any subsequent F_{r+1} or F'_{r+1} is the half-plane solution due to the effective incident field of the preceding diffraction wave from the other edge. When using this direct physical procedure, it is essential to use the fact pointed out earlier (§ 2) that a diffraction wave from an edge is not in general a separate physical entity but has a 'cut-off' and reflected wave associated with it. Thus the solution I (161) applied to the lower half-plane involves the pressures in the incident field for all $y>0$, $x=0$, and when considering $F_1(Y,t)$ as being produced by the incident field of the first diffraction wave from the upper edge we must include the associated cut-off wave as part of this field; this wave leads to the negative p_i term in equation (28). Since F_2, F'_2 and all subsequent waves are produced by incident fields arriving from directly above or below the relevant edge, they have zero associated cut-off and reflected waves and can be considered each as a separate incident field as indicated by the form of equation (29).

Provided the possible effect of associated cut-off waves is borne in mind, this separate consideration of the constituent waves of the effective incident field is possibly simpler in use, since it is easier to think of these waves being separately incident on the second half-plane than to think of the whole scattered field from one half-plane as forming a single incident field. This alternative method will accordingly be used to obtain the solution for the pressure flux ψ through the slit.

3·2. *Solution for* $\psi(y,t)$

We shall limit consideration to the case of a symmetrical incident field, since the extension to the more general case of an unsymmetrical field involves essentially only a duplication of formulae and symbols; this can easily be made for any particular problem.

In the light of the previous discussion of the physical nature of the problem we assume *ab initio* a solution for ψ of the form

$$\psi(y,t) = \psi_i(y,t) + [\Psi_0(y,t) + \Psi_1(y,t) + \ldots + \Psi_r(y,t) + \ldots] + [\Psi_0(y',t) + \Psi_1(y',t) + \ldots + \Psi_r(y',t) + \ldots], \quad (34)$$

in which ψ_i is the pressure gradient in the external incident field p_i, and the bracketed sets of terms give successive diffraction wave contributions from the lower and upper edges.

Thus $\Psi_0(y,t)$ is the pressure gradient in the first diffraction wave due to the external field alone incident on the lower half-plane, and when this Ψ_0 wave reaches the upper edge it produces a diffraction wave contributing an additional $\Psi_1(y',t)$; this Ψ_1 wave then produces $\Psi_2(y,t)$ on reaching the lower edge and so on. Similarly, $\Psi_0(y',t)$ is produced by the external field incident on the upper half-plane, and this Ψ_0 wave then produces in turn $\Psi_1(y,t)$ at the lower edge and so on. Generally, therefore, the contribution Ψ_{r+1} from any edge is produced by an effective incident field of the Ψ_r wave from the other edge.

The relevant solution of paper I for a single half-plane is equation I (165), in which the additional pressure gradient contributed by the diffraction wave is given by an integral involving values of the incident gradient cancelled by the half-plane. We must here note that in paper I, the symbol ψ_0 was used to denote the total pressure gradient in the half-plane problem, since it was this quantity which determined the further diffraction waves in the strip problem. In the present problem of the slit it has been found desirable to use Ψ_0 to denote the pressure gradient in the half-plane problem due to the diffraction wave only, and this will be given by the integral term in I (165). Hence for Ψ_0 we have

$$\Psi_0(y,t) = \frac{1}{\pi}\int_0^\infty \frac{\Psi_i(Y_0, t-y-Y_0)}{y+Y_0}\sqrt{\left(\frac{Y_0}{y}\right)}\,dY_0, \quad (35)$$

where $\Psi_i(Y,t)$ denotes the pressure gradient in the symmetrical external incident field on the lower half-plane.

For the production of $\Psi_1(y,t)$ regarded as the diffraction wave produced at the lower edge by an incident $\Psi_0(y',t)$ wave, we note that the relevant values of the incident gradient lie wholly on the lower half-plane which is outside the regions of cut-off and reflected waves associated with $\Psi_0(y',t)$. Unlike the previous solution for pressure there is thus no need to obtain a special formula for Ψ_1 in terms of Ψ_0, and we proceed direct to the general case of the production of $\Psi_{r+1}(y,t)$ from the lower edge by the $\Psi_r(y',t)$ wave from the upper edge. Since $y' = 1+Y$, the relevant incident gradient which is cancelled by the lower plane is $\Psi_r(1+Y,t)$, whence equation I (165) gives immediately

$$\Psi_{r+1}(y,t) = \frac{1}{\pi}\int_0^\infty \frac{\Psi_r(1+Y_0, t-y-Y_0)}{y+Y_0}\sqrt{\left(\frac{Y_0}{y}\right)}\,dY_0. \quad (36)$$

Equations (34), (35) and (36) give a complete solution for the pressure gradient through the slit when subjected to a symmetrical incident field. From equations (35) and (36) it is easy to obtain relations analogous to (31) and (32) and to show that the solution is unique, subject to the finite velocity of propagation of diffraction effects from the edges. Using this solution for ψ, equations I (7) and I (1) give the formal solution for the pressure field everywhere.

4. Plane $H(t)$ pulse incident normally on a perfectly reflecting screen with a uniform slit

4·1. *Solutions for p_b and ψ*

We consider now the special case of a plane pulse arriving from the right $x>0$ at normal incidence, and we take the time variation in the pulse to be given by Heaviside's unit function $H(t)$ (figure 3). The solution for any other time variation can then be immediately obtained by superposition as in the strip problem of paper I.

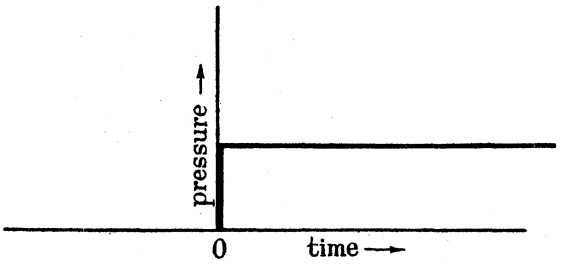

Figure 3. $H(t)$ pulse.

We measure time from the instant at which the pulse arrives at the slit, and the external incident field is thus given by

$$p_i = H(t+x). \tag{37}$$

We note that this field is symmetrical with respect to the slit whence the pressure distribution on the back of the screen will be the same for either half-plane. For the lower half-plane we can then write

$$p_b = F(Y,t) = F_0(Y,t)+F_1(Y,t)+\ldots, \tag{38}$$

where F_0 corresponds to the single half-plane problem and is given by (27) and (37), whilst the subsequent terms are then given by equations (28) and (29) with $F'_r \equiv F_r$ because of symmetry.

In view of the relation (32) it is convenient as in paper I to use a different origin of time for each wave by writing

$$\tau = t-r-Y, \tag{39}$$

so that any term in (38) is zero when its relevant τ is negative.

The first term in (38) can then be written in exactly the same form as for the strip problem, since it is simply the single half-plane solution, namely,

$$F_0(Y,t) \equiv G_0(Y,\tau) = \frac{2}{\pi}\tan^{-1}\sqrt{\left(\frac{\tau}{Y}\right)}\,H(\tau). \tag{40}$$

Since the remaining terms F_1, F_2, ... are all negative we write

$$F_r(Y,t) \equiv -f_r(Y,\tau) \quad (r\geqslant 1), \tag{41}$$

whence equations (28) and (29) with $F'_r \equiv F_r$ give results for $\tau>0$ which can be expressed as

$$f_1(Y,\tau) = G_0(Y,\tau+1)-G_0(Y,1)-\frac{1}{\pi}\int_0^{\frac{1}{2}\tau}\frac{G_0(Y_0,\tau-2Y_0)}{1+Y+Y_0}\sqrt{\left(\frac{Y}{1+Y_0}\right)}\,dY_0, \tag{42}$$

$$f_{r+1}(Y,\tau) = \frac{1}{\pi}\int_0^{\frac{1}{2}\tau}\frac{f_r(Y_0,\tau-2Y_0)}{1+Y+Y_0}\sqrt{\left(\frac{Y}{1+Y_0}\right)}\,dY_0 \quad (r\geqslant 1). \tag{43}$$

The final solution for the pressure on the rear of either half-plane at distance Y from an edge is then

$$p_b = F(Y,t) = G_0(Y,t-Y) - f_1(Y,t-Y-1) - \ldots - f_r(Y,t-Y-r) - \ldots, \tag{44}$$

where for any finite time $t<Y+n+1$, all terms $r>n$ are zero and the solution involves only a finite number of terms.

As a special limiting case we may here note that for a point on the rear of either half-plane at a large distance from the slit, the pressure in the initial stages when $(t-Y)/Y$ is small is given from (40) to (44), with $Y\to\infty$ and $t-Y$ finite, by

$$p_b \to \frac{1}{\sqrt{Y}}\left\{\frac{2}{\pi}\sqrt{(t-Y)} - A_1(t-Y-1) - A_2(t-Y-2) - \ldots\right\} \quad (Y\to\infty), \tag{45}$$

$$A_1(\tau) = \frac{2}{\pi}[\sqrt{(\tau+1)}-1] - \frac{1}{\pi}\int_0^{\frac{1}{2}\tau} \frac{G_0(Y_0,\tau-2Y_0)}{\sqrt{(1+Y_0)}}\,dY_0, \tag{46}$$

$$A_{r+1}(\tau) = \frac{1}{\pi}\int_0^{\frac{1}{2}\tau} \frac{A_r(Y_0,\tau-2Y_0)}{\sqrt{(1+Y_0)}}\,dY_0 \quad (r\geqslant 1). \tag{47}$$

The solution for the pressure gradient $\psi(y,t)$ in the slit can similarly be obtained by using the form (37) for the external incident field in the general solution for any field given by (34), (35) and (36). For this second form of solution of the problem we can use a different origin of time for each diffraction wave by writing

$$\tau' = t-y-r, \quad \Psi_r(y,t) \equiv g_r(y,\tau'). \tag{48}$$

The solution for the gradient ψ can then be expressed in the form

$$\begin{aligned}\psi(y,t) = \delta(t) &+ [g_0(y,t-y) + g_1(y,t-y-1) + \ldots] \\ &+ [g_0(y,t-\overline{1-y}) + g_1(y,t-1-\overline{1-y}) + \ldots],\end{aligned} \tag{49}$$

where the Dirac function $\delta(t)$ is the gradient in the external $H(t)$ pulse, whilst the g_r functions are given by

$$g_0(y,\tau') = \frac{1}{\pi(\tau'+y)}\sqrt{\left(\frac{\tau'}{y}\right)}\,H(\tau'), \tag{50}$$

$$g_{r+1}(y,\tau') = \frac{1}{\pi}\int_0^{\frac{1}{2}\tau'} \frac{g_r(1+Y_0,\tau'-2Y_0)}{y+Y_0}\sqrt{\left(\frac{Y_0}{y}\right)}\,dY_0. \tag{51}$$

Any g_r function is zero for $\tau'<0$, so that the solution (49) consists only of a finite number of terms for any finite time t.

The preceding solutions for p_b and ψ are each separately sufficient to give the complete pressure field in conjunction with equation I (1) and either equation I (9) or I (7).

4·2. *Pressure flux/unit length through slit and total force/unit length on back of screen*

If we consider unit length in the z direction, a quantity $Q(t)$ can be defined by

$$Q(t) = \int_0^1 \left(\frac{\partial p}{\partial x}\right)_{x=0} dy = \int_0^1 \psi(y,t)\,dy, \tag{52}$$

If we replaced p in this equation by velocity potential the corresponding quantity would be the flux/unit length as usually defined. By analogy, $Q(t)$ will be referred to as the 'pressure flux' through the slit.

The corresponding total force/unit length P_b on the back of the screen, i.e. on both half-planes together, is given by

$$P_b = 2\int_0^\infty F(Y,t)\,dY. \tag{53}$$

Now, by an argument exactly similar to that in § 3·6 of paper I, we can show that the integrated pressure over any plane $x = -X < 0$ is propagated to the rear as a plane wave, and in particular we can then obtain an equation similar to I (102) but with interchanged ranges of integration, namely,

$$\int_C^B \frac{\partial}{\partial x}(p-p_i)\,dy = \int_D^C \frac{1}{c}\frac{\partial p_b}{\partial t}\,dy + \int_B^A \frac{1}{c}\frac{\partial p_b}{\partial t}\,dy, \tag{54}$$

where the points A and D (figure 2) lie beyond the pressure front of the diffraction regions at any time.

Physically therefore we have a result, similar to that of paper I, that the excess flux through the slit is proportional to the total force on the back of the screen. In the present non-dimensional units with $H(t)$ shape of pulse we can write equation (54), by use of (52) and (53), in the form

$$Q(t) - \delta(t) = \frac{dP_b}{dt}, \tag{55}$$

which is analogous to equation I (105) of the strip problem.

Similarly, in the first two intervals of time up to $t = 2$ we can obtain explicit formulae for P_b and Q analogous to results obtained in § 3·6 of paper I for the strip problem. It may here be noted that the formulae derived in paper I for the average pressure on the back of the strip apply equally to the total force/unit length on the back of the strip since the width of the strip was taken as unity.

We now consider separately the first two unit intervals of time.

(i) $0 \leqslant t < 1$

For this first interval, P_b is exactly equal to the corresponding total force/unit length on the back in the strip problem, since in both problems this total force is simply twice the force on a single half-plane subjected to the $H(t)$ pulse. Corresponding to equation I (109), we obtain in the slit problem

$$P_b = t \quad (0 \leqslant t < 1), \tag{56}$$

and then from (55) we have

$$Q(t) = \delta(t) + 1 \quad (0 \leqslant t < 1). \tag{57}$$

(ii) $1 \leqslant t < 2$

For this interval, P_b involves values of F_0 and F_1, the contribution from the former being given by (56) as in the first interval. The contribution of F_1 is most easily obtained by using the Laplace transformation. Thus, if we write

$$\Delta_0(Y,\lambda) = \int_0^\infty e^{-\lambda t} F_0(Y,t)\,dt, \quad \Phi_1(Y,\lambda) = \int_0^\infty e^{-\lambda t} F_1(Y,t)\,dt, \tag{58}$$

then Δ_0 is given by equation I (76) which can be written by use of I (51) and change of integration variable in the form

$$\Delta_0(Y,\lambda) = \frac{2}{\pi\lambda}\int_0^{\frac{1}{2}\pi} e^{-\lambda Y \sec^2\theta}\, d\theta. \tag{59}$$

We now apply the Laplace transformation to equation (28), after putting $F' \equiv F$ by virtue of symmetry, and we obtain

$$\Phi_1(Y,\lambda) = \frac{1}{\pi}\int_0^{\infty} \frac{e^{-\lambda(1+Y+Y')}}{1+Y+Y'}\left[\Delta_0(Y',\lambda) - \frac{1}{\lambda}\right]\sqrt{\left(\frac{Y}{1+Y'}\right)}\, dY'. \tag{60}$$

Hence, if we integrate with respect to Y from 0 to ∞, interchange orders of integration and then change from Y to ϕ as integration variable by the substitution $Y = (Y'+1)\tan^2\phi$, we find

$$\int_0^{\infty} \Phi_1(Y,\lambda)\, dY = \frac{2}{\pi}\int_0^{\infty}\left[\Delta_0(Y',\lambda) - \frac{1}{\lambda}\right]\int_0^{\frac{1}{2}\pi} e^{-\lambda(Y'+1)\sec^2\phi}\tan^2\phi\, d\phi\, dY'. \tag{61}$$

From equation (59), we can now write

$$\Delta_0(Y',\lambda) - \frac{1}{\lambda} = \frac{2}{\pi\lambda}\int_0^{\frac{1}{2}\pi}(e^{-\lambda Y'\sec^2\theta} - 1)\, d\theta$$

in equation (61) and interchange orders of integration to perform the Y' integration with the result

$$\int_0^{\infty} \Phi_1(Y,\lambda)\, d\lambda = -\frac{4}{\pi^2\lambda^2}\int_0^{\frac{1}{2}\pi}\int_0^{\frac{1}{2}\pi} \frac{e^{-\lambda\sec^2\phi}\sin^2\phi\sec^2\theta}{\sec^2\phi + \sec^2\theta}\, d\theta\, d\phi. \tag{62}$$

The θ integration can now be performed, and then making a final substitution $\sec^2\phi = \sec\eta$ we find

$$2\int_0^{\infty} \Phi_1(Y,\lambda)\, dY = -\frac{2}{\pi\lambda^2}\int_0^{\frac{1}{2}\pi} e^{-\lambda\sec\eta}(1-\cos\eta)\, d\eta. \tag{63}$$

This is the same as the second term in equation I (113) save for one difference in sign, and the interpretation of (63) is therefore the same as the bracketed terms in I (114) apart from relevant changes of sign. Thus allowing for the contribution of the F_0 term as given by (56) we obtain finally

$$P_b = t - \frac{2}{\pi}[\zeta\sec\zeta - \tan\zeta + \zeta - \log(\sec\zeta + \tan\zeta)] \quad (1 \leqslant t < 2), \tag{64}$$

where

$$\sec\zeta = t. \tag{65}$$

It will be noted that this expression differs only in the signs of the second and third terms from the corresponding equation I (114) of the strip problem. Similarly, equations I (117) and I (118) will give the total impulse/unit length in the slit problem if we replace $\bar{p}_b$ by P_b and change the signs of the second and fourth bracketed terms in I (118).

The formula for $Q(t)$ in this second interval can be obtained from (64) by using (55), with $\delta(t)$ neglected since it is zero for $t > 0$. We then find

$$Q(t) = 1 - \frac{2}{\pi}(\zeta - \sin\zeta) \quad (1 \leqslant t < 2), \tag{66}$$

with ζ defined by (65).

4·3. *Asymptotic solution and approximate formulae*

Since the preceding solutions in the form of diffraction waves are not convenient when many waves are involved, it is desirable to obtain an alternative form for large values of t. Such an asymptotic form of solution can be derived as in paper I by considering the problem when transformed by the Laplace transformation and making analogous assumptions to those used in Rayleigh's approximate method for a sinusoidal wave train of long wavelength (Lamb 1932, p. 532). Alternatively, equivalent direct assumptions can be made in the actual problem which lead to the same final solution. We shall follow this alternative direct method since it is perhaps physically more instructive.

First, for any point $(-X, y, 0)$ to the rear of the slit at a large distance R from the centre-line of the slit, we should expect the slit to behave as a two-dimensional source when $t-R$ is large, i.e. after the initial effects of the sharp front in the external incident pulse have been evened out.

For such a point, the exact equation I (7) with the surface integral taken over the slit, can be written in view of (14) as

$$p(t, -X, y) = \frac{1}{\pi}\int_0^\infty \int_0^1 \frac{1}{r}\psi(y_0, t-r)\, dy_0\, dz_0, \tag{67}$$

where

$$r^2 = X^2 + (y-y_0)^2 + z_0^2. \tag{68}$$

The assumption of a two-dimensional source then corresponds to neglecting in (67) the variation of r with y_0 when both r and $t-r$ are large. Hence, writing

$$R^2 = X^2 + (y-\tfrac{1}{2})^2, \quad r_0^2 = R^2 + z_0^2, \tag{69}$$

and replacing r in (67) by its value r_0 on the centre-line of the slit, we can perform the y_0 integration in terms of the pressure flux $Q(t)$ to obtain

$$p(t, -X, y) \sim \frac{1}{\pi}\int_0^\infty \frac{Q(t-r_0)}{r_0}\, dz_0 \quad (t-R \text{ large}, \ R \text{ large}). \tag{70}$$

If we now change the integration variable by writing

$$z_0 = R\sinh u, \quad r_0 = R\cosh u, \tag{71}$$

equation (70) takes the more usual form for a wave from a two-dimensional source, namely,

$$p(t, -X, y) \sim \frac{1}{\pi}\int_0^\infty Q(t-R\cosh u)\, du \quad (t-R \text{ large}, \ R \text{ large}). \tag{72}$$

As a second assumption, when t is large it seems reasonable to expect that the flow near the slit will become approximately incompressible throughout a region round the slit, and that this region will increase in size with increasing time. In particular, when t is large enough this region of sensibly incompressible flow will include points at large distance R from the centre-line of the slit.

The relevant pressure flux is $Q(t)$, and the pressure in the slit is unity by virtue of equation I (2) and (37); hence, the known solution (Lamb 1932, p. 73) for incompressible flow through a slit gives on this second assumption:

$$p(t, -X, y) \sim 1 - \frac{Q(t)}{\pi}\log 4R \quad (t/R \text{ large}, \ R \text{ large}). \tag{73}$$

But when R and t/R are both large, equations (72) and (73) can apply simultaneously, whence we obtain

$$\frac{1}{\pi}\int_0^\infty Q(t-R\cosh u)\,du+\frac{Q(t)}{\pi}\log 4R\sim 1 \quad (t/R \text{ large}, R \text{ large}). \tag{74}$$

This gives an integral equation to determine the asymptotic form of $Q(t)$. It can be solved by writing

$$\overline{Q}(\lambda)=\int_0^\infty \mathrm{e}^{-\lambda t}\,Q(t)\,dt, \tag{75}$$

and applying the Laplace transformation to obtain

$$\frac{\overline{Q}}{\pi}\{K_0(\lambda R)+\log 4R\}\sim 1 \quad (\lambda R \text{ small}, R \text{ large}), \tag{76}$$

in which it may be noted that the condition λR small follows from the condition t/R large.

But for λR small we can write (Whittaker & Watson 1927, p. 374)

$$K_0(\lambda R)\sim -\log(\tfrac{1}{2}\lambda R)-\gamma, \tag{77}$$

and on substitution in (76) we obtain

$$\overline{Q}(\lambda)\sim\frac{-\pi}{\lambda(\log\lambda-\log 8+\gamma)} \quad (\lambda \text{ small}). \tag{78}$$

This equation is the analogue of the corresponding result (Lamb 1932, p. 532, equation (20)) for the sinusoidal wave train of long wave-length.

The interpretation of (78) by the Bromwich integral is straightforward, employing the usual contour (Carslaw & Jaeger 1941, figure 11) for a function with a branch point at the origin in the complex λ plane; we find

$$Q(t)\sim\int_0^\infty\frac{\pi\,\mathrm{e}^{-\beta t\xi}}{\xi\{\pi^2+(\log\xi)^2\}}\,d\xi \quad (t \text{ large}), \tag{79}$$

where

$$\beta=8\,\mathrm{e}^{-\gamma}=4{\cdot}492. \tag{80}$$

For numerical evaluation of this asymptotic form for Q it was found convenient to write it in the form

$$Q(t)\sim\int_0^\pi \mathrm{e}^{-\beta t\xi}\,d\theta, \quad \xi=\mathrm{e}^{-\pi\cot\theta} \quad (t \text{ large}). \tag{81}$$

The assumptions made in the derivation of the preceding asymptotic solution for $Q(t)$ can also be applied separately to obtain approximate forms for the pressure at points to the rear. We can summarize these approximations for large time by considering different regions to the rear proceeding outwards from the slit.

(a) t large, t/R large

In this region the flow is sensibly incompressible, and from the known solution for such flow (Lamb 1932, p. 73) we can write

$$p(t,-X,y)\sim 1-\frac{Q(t)}{\pi}\xi(x,y), \tag{82}$$

where

$$X=\tfrac{1}{2}\sinh\xi\sin\eta, \quad y=\tfrac{1}{2}+\tfrac{1}{2}\cosh\xi\cos\eta. \tag{83}$$

In particular, for a point on the rear of a half-plane at distance Y from the edge we have

$$p_b \sim 1-\frac{Q(t)}{\pi}\cosh^{-1}(1+2Y) \quad (t \text{ large}, t/(Y+\tfrac{1}{2}) \text{ large}). \tag{84}$$

Similarly, for a point to the rear in the plane of symmetry, $y=\frac{1}{2}$, the solution (82) simplifies to

$$p(t,-X,\tfrac{1}{2}) \sim 1-\frac{Q(t)}{\pi}\sinh^{-1}2X \quad (t \text{ large}, t/X \text{ large}). \tag{85}$$

In these equations (82), (84) and (85) we can use values for $Q(t)$ given by the asymptotic solution (81).

When t is large enough, this innermost region contains points for which R is large compared with the unit width of the slit. For such points we can approximate further in (82) to obtain the form (73) already used in the derivation of the asymptotic form for $Q(t)$, namely,

$$p(t,-X,y) \sim 1-\frac{Q(t)}{\pi}\log 4R, \quad (t/R \text{ large}, R \text{ large}). \tag{73 bis}$$

(b) R large, $t-R$ large

These conditions are those necessary for the slit to behave effectively as a simple two-dimensional source, and the pressure is therefore given by equation (70) or its equivalent equation (72).

If we use $Q(t)=0$ for $t<0$ and change the integration variable in (70) to r_0, we can write the approximation in the third form

$$p(t,-X,y) \sim \frac{1}{\pi}\int_R^t \frac{Q(t-r_0)}{\sqrt{(r_0^2-R^2)}}\,dr_0 \quad (R \text{ large}, t-R \text{ large}). \tag{86}$$

When R is very large so that $t-R$ can be large but $(t-R)/R$ small, we can approximate further to equation (86) and write

$$\left.\begin{aligned} p(t,-X,y) &\sim \frac{Q_1(t-R)}{\sqrt{R}}, \\ Q_1(t) &= \frac{1}{\pi}\int_0^t \frac{Q(t-\mu)}{\sqrt{(2\mu)}}\,d\mu, \end{aligned}\right\} \quad (t-R \text{ large}, (t-R)/R \text{ small}). \tag{87}$$

For a point of very large R the approximation (86) will become valid when $t-R$ becomes large and will in fact remain valid thereafter. However, in the early stages of its validity it will be simpler to use the form (87), whilst ultimately the more convenient solution (73) becomes valid.

It will be noted that the form (86) and its special case (87) involve arguments of Q from 0 to $t-R$, but, in general, these forms are only strictly valid when the contributions from large arguments predominate. The asymptotic solution for Q could thus be used over the whole range of integration, but rather better accuracy is to be expected if we use the exact forms (57) and (66) for the relevant arguments of Q and the asymptotic form (81) for greater arguments only.

For the special case of a point at a large distance to the rear which is on or near the plane of symmetry $y=\frac{1}{2}$ bisecting the slit, the forms (86) and (87) become valid at relatively early times. Thus for a point $y=\frac{1}{2}$, $x=-X$ where X is large, the variation of r with y_0 in

the exact equation (67) is small in absolute magnitude of order $1/8r_0$. We can therefore neglect this variation to obtain (86) and (87), not only when $t-X$ is large but more generally provided only that $t-X$ is not small.

For such a point equation (87) will then hold in particular within the range $t-X<1$, except for small $(t-X)$, and substituting the solution (57) for $Q(t)$ we find

$$p(t,-X,\tfrac{1}{2}) \sim \frac{1}{\pi\sqrt{X}}\left[\frac{1}{\sqrt{[2(t-X)]}}+\sqrt{[2(t-X)]}\right] \quad (1>t-X \text{ not small}), \tag{88}$$

for a point on the plane of symmetry at large distance X to the rear.

4·4. *Pressure at any point to the rear prior to arrival of second diffraction wave from nearer edge*

If r_1 and r_2 $(\geqslant r_1)$ denote the distances of any point from the edges of the half-planes then considering, in view of symmetry, only points $(-X,y,0)$ below the plane of symmetry we have

$$r_1^2 = X^2+y^2, \quad r_2^2 = X^2+(1-y)^2 = X^2+(1+Y)^2. \tag{89}$$

Now the interaction between the half-planes does not start until time $t=1$, and up to time $t=r_1+1$ the pressure at a point to the rear may be obtained simply by a superposition of results for the single half-plane as given by Friedlander (1946).

For a point in the shadow the pressure is the sum of the contributions from the first diffraction wave from either edge and may be written

$y=-Y<0$, $t<r_1+1$:

$$p(t,-X,y) = \tfrac{1}{2}[G_0(r_1-X,t-r_1)+G_0(r_1+X,t-r_1)] - \tfrac{1}{2}[G_0(r_2-X,t-r_2)-G_0(r_2+X,t-r_2)], \tag{90}$$

where G_0 is the function already defined by equation (40).

For a point in the direct line of the slit we have the direct contribution of the external incident pulse added to the diffraction wave contributions and the pressure is given by

$0<y\leqslant\frac{1}{2}$, $t<r_1+1$:

$$p(t,-X,y) = H(t-X)-\tfrac{1}{2}[G_0(r_1-X,t-r_1)-G_0(r_1+X,t-r_1)] - \tfrac{1}{2}[G_0(r_2-X,t-r_2)-G_0(r_2+X,t-r_2)]. \tag{91}$$

On the edge of the shadow $y=0$, the two forms (90) and (91) are equivalent, since the change of sign in the first G_0 term balances the additional contribution of the incident pulse in (91).

For a point on the plane of symmetry, $y=\frac{1}{2}$, when X is large we have

$$r_1 = r_2 \sim X+\frac{1}{8X}, \tag{92}$$

and using (40) for G_0 we obtain approximately

X *large*, $\dfrac{1}{8X}<t-X<1$:

$$p(t,-X,\tfrac{1}{2}) \sim \frac{2}{\pi}\tan^{-1}\frac{1}{\sqrt{[8X(t-X)]}}+\frac{2}{\pi}\sqrt{\frac{t-X}{2X}}. \tag{93}$$

When $t-X$ is not small, $8X(t-X)$ is large and we can drop the $\tan^{-1}$ symbol in the first term to obtain the result (88) corresponding to the behaviour of the slit as a simple source.

It will be noted that as $t-X$ increases, the first term in (93) decreases whilst the second increases, and the pressure has in fact a minimum, within the range of validity of (93), given approximately by

$$p_{\text{min.}} \sim \frac{2}{\pi\sqrt{X}} \quad \text{at} \quad t-X \sim \tfrac{1}{2}. \tag{94}$$

4·5. *Discussion of numerical results for plane $H(t)$ pulse at normal incidence*

4·51. *Pressure-time variation at points on the back of the screen*

The pressure p_b on the back of either half-plane has been evaluated at points distant $Y = 0(0{\cdot}2)4$ from the edge for times $t = 0(0{\cdot}2)4$. The relevant values of G_0 are given in tables 1*a* and 1*b* which were calculated from equation (40) to an accuracy of three units or better in the fourth decimal place. The function f_1 was evaluated from equation (42) for intervals of 0·2 in τ by numerical integration using an interval of 0·1 in Y_0; for this purpose, values of G_0 given in paper I for $Y = 0{\cdot}1$, 0·3, etc., were used in addition to the values of G_0 now quoted. The results for f_1 are given in tables 2*a* and 2*b*, in which any value is unlikely

TABLE 1*a*. VALUES OF $G_0\,(Y, \tau)$ FOR $0 < Y \leqslant 2$

τ \ Y	0·2	0·4	0·6	0·8	1·0	1·2	1·4	1·6	1·8	2·0
0	0	0	0	0	0	0	0	0	0	0
0·2	0·5	0·3918	0·3333	0·2952	0·2677	0·2468	0·2300	0·2164	0·2048	0·1950
0·4	0·6082	0·5	0·4360	0·3918	0·3590	0·3333	0·3125	0·2952	0·2804	0·2679
0·6	0·6667	0·5642	0·5	0·4544	0·4195	0·3918	0·3689	0·3498	0·3333	0·3188
0·8	0·7047	0·6082	0·5457	0·5	0·4645	0·4360	0·4120	0·3918	0·3743	0·3590
1·0	0·7321	0·6411	0·5805	0·5355	0·5	0·4710	0·4467	0·4258	0·4077	0·3918
1·2	0·7531	0·6667	0·6082	0·5642	0·5288	0·5	0·4754	0·4543	0·4358	0·4195
1·4	0·7697	0·6875	0·6309	0·5880	0·5532	0·5244	0·5	0·4788	0·4601	0·4436
1·6	0·7837	0·7047	0·6500	0·6082	0·5742	0·5457	0·5212	0·5	0·4813	0·4645
1·8	0·7951	0·7194	0·6667	0·6257	0·5923	0·5642	0·5399	0·5187	0·5	0·4833
2·0	0·8053	0·7321	0·6812	0·6411	0·6082	0·5805	0·5564	0·5355	0·5167	0·5
2·2	0·8136	0·7436	0·6939	0·6544	0·6223	0·5950	0·5713	0·5505	0·5319	
2·4	0·8212	0·7531	0·7047	0·6667	0·6350	0·6082	0·5847	0·5642		
2·6	0·8276	0·7620	0·7148	0·6776	0·6466	0·6202	0·5970			
2·8	0·8340	0·7700	0·7240	0·6875	0·6570	0·6309				
3·0	0·8391	0·7771	0·7323	0·6966	0·6667					
3·2	0·8442	0·7837	0·7398	0·7047						
3·4	0·8486	0·7897	0·7468							
3·6	0·8524	0·7951								
3·8	0·8564									

TABLE 1*b*. VALUES OF $G_0\,(Y, \tau)$ FOR $2 < Y < 4$

τ \ Y	2·2	2·4	2·6	2·8	3·0	3·2	3·4	3·6	3·8
0	0	0	0	0	0	0	0	0	0
0·2	0·1864	0·1788	0·1724	0·1660	0·1609	0·1558	0·1514	0·1474	0·1436
0·4	0·2564	0·2469	0·2380	0·2300	0·2229	0·2163	0·2103	0·2049	
0·6	0·3061	0·2953	0·2852	0·2760	0·2677	0·2602	0·2532		
0·8	0·3456	0·3333	0·3224	0·3125	0·3034	0·2953			
1·0	0·3777	0·3650	0·3534	0·3430	0·3333				
1·2	0·4050	0·3918	0·3798	0·3689					
1·4	0·4287	0·4153	0·4030						
1·6	0·4495	0·4358							
1·8	0·4681								

to be in error by more than 0·0005. In table 2*a*, the values for $Y = 0{\cdot}1$, 0·3, etc., are less extensive than for $Y = 0{\cdot}2$, 0·4, etc., since the former were required only in the subsequent determination of f_2 from equation (43) by numerical integration. The values obtained for f_2 are given in table 3 to an accuracy of about 0·0001.

To obtain values of p_b in the range $0 \leqslant Y \leqslant 1$ at times $3 < t \leqslant 4$, the function f_3 is also required, but it was found that all relevant values were zero to four decimal places and therefore negligible relative to potential errors in the earlier functions.

TABLE 2*a*. VALUES OF $f_1\ (Y, \tau)$ FOR $0 < Y \leqslant 1$

τ \ Y	0·1	0·2	0·3	0·4	0·5	0·6	0·7	0·8	0·9	1·0
0	0	0	0	0	0	0	0	0	0	0
0·2	0·0116	0·0151	0·0168	0·0184	0·0193	0·0200	0·0205	0·0208	0·0211	0·0208
0·4	0·0195	0·0254	0·0287	0·0314	0·0334	0·0344	0·0355	0·0360	—	0·0364
0·6	0·0254	0·0337	0·0382	0·0416	0·0443	0·0458	0·0475	0·0482	—	0·0494
0·8	0·0297	0·0400	0·0456	0·0499	0·0535	0·0556	—	0·0585	—	0·0601
1·0	0·0338	0·0455	0·0517	0·0567	0·0605	0·0635	—	0·0670	—	0·0690
1·2	0·0368	0·0494	0·0568	0·0627	—	0·0702	—	0·0740	—	0·0766
1·4	0·0389	0·0530	0·0610	0·0670	—	0·0753	—	0·0803	—	0·0831
1·6	0·0411	0·0556	—	0·0711	—	0·0800	—	0·0866	—	0·0889
1·8	0·0430	0·0584	—	0·0746	—	0·0843	—	0·0902	—	0·0939
2·0	—	0·0602	—	0·0774	—	0·0878	—	0·0942	—	0·0983
2·2	—	0·0621	—	0·0799	—	0·0907	—	0·0975	—	—
2·4	—	0·0636	—	0·0821	—	0·0934	—	—	—	—
2·6	—	0·0645	—	0·0838	—	—	—	—	—	—
2·8	—	0·0658	—	—	—	—	—	—	—	—

TABLE 2*b*. VALUE OF $f_1\ (Y, \tau)$ FOR $1 < Y \leqslant 3$

τ \ Y	1·2	1·4	1·6	1·8	2·0	2·2	2·4	2·6	2·8	3·0
0	0	0	0	0	0	0	0	0	0	0
0·2	0·0211	0·0208	0·0208	0·0205	0·0202	0·0199	0·0195	0·0193	0·0189	
0·4	0·0367	0·0366	0·0367	0·0363	0·0359	0·0353	0·0349	0·0345		
0·6	0·0499	0·0499	0·0499	0·0496	0·0491	0·0485	0·0478			
0·8	0·0610	0·0611	0·0612	0·0610	0·0606	0·0599				
1·0	0·0703	0·0706	0·0711	0·0707	0·0704					
1·2	0·0782	0·0789	0·0795	0·0794						
1·4	0·0852	0·0860	0·0869							
1·6	0·0913	0·0924								
1·8	0·0964									

TABLE 3. VALUES OF $f_2\ (Y, \tau)$ FOR $0 < Y \leqslant 2$

τ \ Y	0·2	0·4	0·6	0·8	1·0	1·2	1·4	1·6	1·8	2·0
0	0	0	0	0	0	0	0	0	0	0
0·2	0·0000	0·0000	0·0000	0·0000	0·0000	0·0000	0·0000	0·0000	0·0000	
0·4	0·0001	0·0001	0·0002	0·0002	0·0002	0·0002	0·0002	0·0002		
0·6	0·0003	0·0004	0·0005	0·0005	0·0005	0·0005	0·0005			
0·8	0·0006	0·0008	0·0009	0·0009	0·0009	0·0009				
1·0	0·0010	0·0012	0·0013	0·0014	0·0014					
1·2	0·0014	0·0018	0·0019	0·0020						
1·4	0·0018	0·0023	0·0025							
1·6	0·0023	0·0029								
1·8	0·0028									

The general trend in the calculations, that for given small τ and given Y the functions f_1, f_2, f_3 form a rapidly decreasing sequence, corresponds to the result easily obtained from equations (40), (42) and (43) that

$$f_r(Y,\tau) \sim C_r \frac{\sqrt{Y}}{1+Y} \tau^{\frac{1}{2}(3r-1)} \quad (\tau \text{ small}). \tag{95}$$

In addition to the increasing index of τ it may also be shown that as r increases the constant C_r decreases rapidly. It may be noted that the decrease of f_r with increasing r for small τ is more rapid than the corresponding decrease of the analogous G_r functions of the strip problem of paper I.

Using tables 1 *a* to 3, the pressure p_b can be determined from equation (44) for $Y = 0(0{\cdot}2)4$ at times $t = 0(0{\cdot}2)4$. As this final step of the calculations is so simple and since the pressure-time variation is found to be essentially similar in character at all these points, values of p_b are quoted in table 4 for a few typical points only. These values are estimated to be correct to about 0·001 or better.

The limiting case, $Y \to \infty$, of points very distant from the slit has also been examined numerically by using equations (45) to (47) for times $t - Y = 0(0{\cdot}2)3$. Values of A_1, A_2 and $p\sqrt{Y}$ are given in table 5 to estimated accuracies of 0·001 for A_1, 0·0003 for A_2 and 0·002 for $p\sqrt{Y}$.

Finally, the total force P_b on the back of both half-planes in the early stages has been calculated as given in table 6 to an accuracy of about 0·001. For $t \leqslant 2$, these values were obtained by using equations (56), (64) and (65). For $t > 2$, equation (64) was used to give the G_0 and f_1 contributions, whilst the f_2 contribution was obtained by numerical integration of the relevant values of table 3.

TABLE 4. PRESSURE AT POINTS ON BACK OF EITHER HALF-PLANE

t	$Y=0{\cdot}2$	$Y=1$	t	$Y=0{\cdot}2$	$Y=1$	$Y=2$
0	0	0	2·0	0·755	0·5	0
0·2	0	0	2·2	0·760	0·508	0·195
0·4	0·5	0	2·4	0·764	0·517	0·268
0·6	0·608	0	2·6	0·768	0·525	0·319
0·8	0·667	0	2·8	0·772	0·532	0·359
1·0	0·705	0	3·0	0·775	0·539	0·392
1·2	0·732	0·268	3·2	0·778	0·546	0·399
1·4	0·738	0·359	3·4	0·781	0·552	0·408
1·6	0·744	0·420	3·6	0·783	0·557	0·415
1·8	0·750	0·465	3·8	0·786	0·562	0·423
			4·0	0·788	0·567	0·430

TABLE 5. VALUES OF A_1, A_2 AND $\sqrt{Y}\,p_b$, $Y \to \infty$

$t-Y$	$A_1(t-Y-1)$	$\sqrt{Y}\,p_b$	$t-Y$	$A_1(t-Y-1)$	$A_2(t-Y-2)$	$\sqrt{Y}\,p_b$
0	0	0	1·6	0·1169	0	0·688
0·2	0	0·285	1·8	0·1489	0	0·705
0·4	0	0·403	2·0	0·1789	0	0·721
0·6	0	0·493	2·2	0·2071	0·0000	0·737
0·8	0	0·569	2·4	0·2338	0·0004	0·752
1·0	0	0·637	2·6	0·2591	0·0010	0·766
1·2	0·0449	0·653	2·8	0·2833	0·0020	0·780
1·4	0·0823	0·671	3·0	0·3065	0·0032	0·793

TABLE 6. VALUES OF P_b

t	P_b	t	P_b	t	P_b
0	0	1·4	1·391	2·8	2·624
0·2	0·2	1·6	1·579	3·0	2·788
0·4	0·4	1·8	1·762	3·2	2·950
0·6	0·6	2·0	1·941	3·4	3·110
0·8	0·8	2·2	2·116	3·6	3·269
1·0	1·0	2·4	2·288	3·8	3·426
1·2	1·198	2·6	2·457	4·0	3·581

The general nature of the pressure-time curve at individual points on the back of either half-plane is illustrated by the full curves in figure 4. For comparison, the corresponding pressure at the back of a single half-plane subjected to the same external pulse is shown by the broken curves in figure 4; it is seen that the main effect of the second half-plane is simply a slowing down of the asymptotic approach of the pressure to its ultimate value of unity corresponding to complete equalization. It may be noted that on arrival of the second diffraction wave f_1 at time $t = Y+1$, the pressure-time curve decreases in slope discontinuously on account of the initial finite slope of the f_1 wave as indicated by equation (95). Since the following diffraction waves all have zero initial slope, the slope of the pressure-time curve remains continuous at subsequent times.

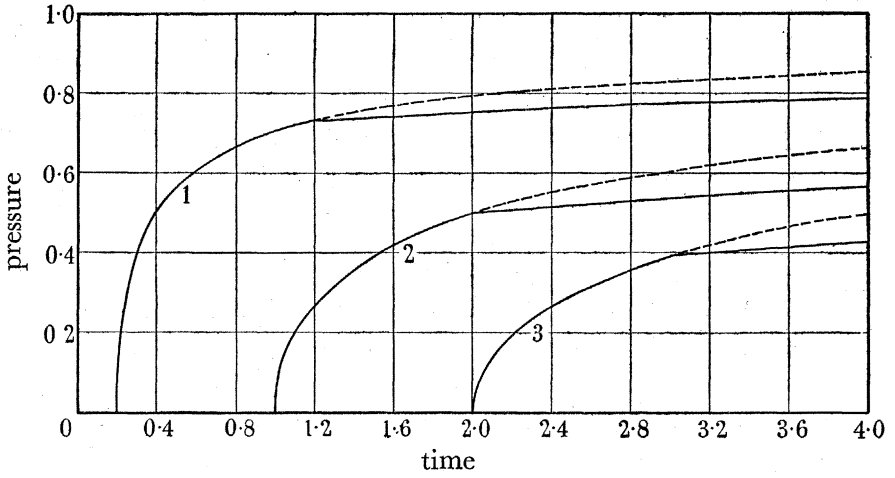

FIGURE 4. Pressure-time variation at points on back of either half-plane. Curve 1, $Y = 0{\cdot}2$. Curve 2, $Y = 1$. Curve 3, $Y = 2$. — slit; --- single half-plane.

For distant points, $Y \to \infty$, the values in table 5 can be plotted, but the resulting pressure-time variation is of exactly similar type to the full curves of figure 4 and exhibits no additional points of interest.

From table 6 the total force/unit length P_b can be plotted against time as shown in figure 5. Up to time $t = 1$ the total force/unit length increases linearly and thereafter at steadily decreasing rate. Ultimately, $P_b \to \infty$ with increasing time, corresponding to virtual equalization of the incident pressure over a steadily increasing area of the half-planes.

4·52. *Pressure-time variation at points to the rear of the screen*

The most interesting features of pressure-time variation occur for points to the rear in the direct line of the slit, i.e. for $0 \leqslant y \leqslant 1$. To illustrate these features, values of pressure have been calculated in the initial stage from equations (90) and (91) for selected points all at

distance $R = 2{\cdot}5$ from the centre line of the slit. These values are shown plotted in figure 6, where figure 6*a* indicates the points to which the curves refer. For the point P on the plane of symmetry, the pressure rises instantaneously to the value of unity corresponding to direct propagation of the incident pulse and remains constant until the first diffraction waves arrive simultaneously from the two edges. The pressure then decreases sharply and reaches a minimum value, after which it commences to increase and will presumably thereafter increase asymptotically to a final value of unity again.

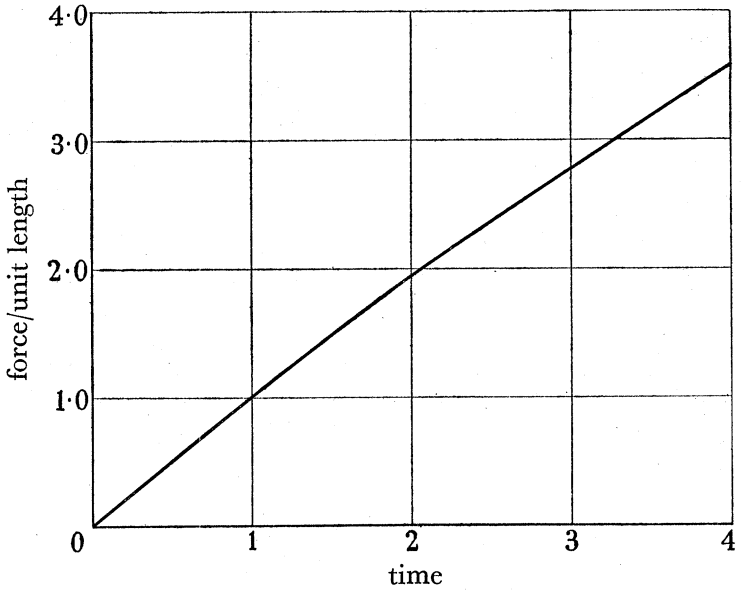

FIGURE 5. Total force on back of half-planes per unit length of slit.

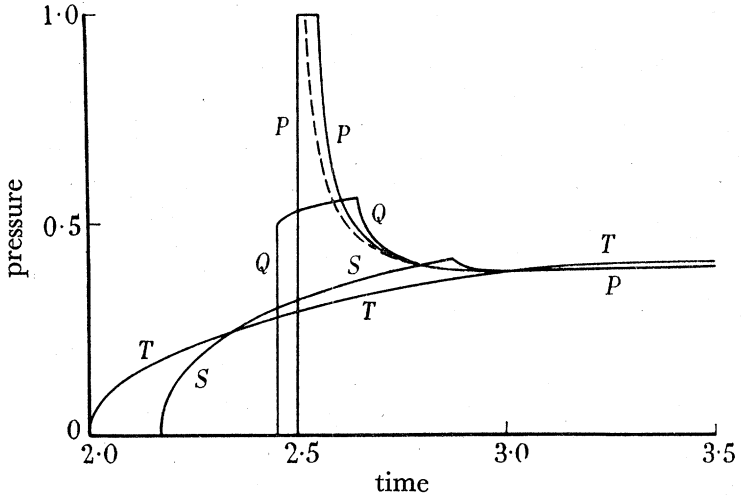

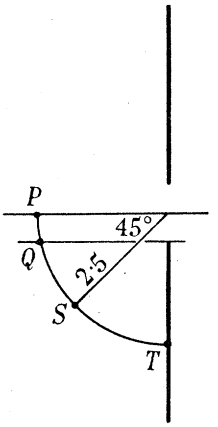

FIGURE 6*a*

FIGURE 6. Pressure-time curves at points to rear distant $R = 2{\cdot}5$ from centre of slit (figure 6*a*).

For the point Q at the edge of the shadow the process is very similar save that here the first 'cut-off' effect of the lower half-plane arrives simultaneously with the direct incident pulse and cancels half the incident peak; the initial sharp rise of pressure at Q is thus only one-half that in the incident pulse. The pressure then increases at Q until the first diffraction wave from the upper edge arrives; this causes the pressure to decrease and subsequently pass through a minimum before commencing to increase steadily again. By time $t = 2{\cdot}7$,

the curve for this point Q effectively coincides in figure 6 with the curve for the point P since the calculated pressures differ by 0·001 or less.

For the point S at 45° in the shadow, there is no initial sharp rise, since only diffraction effects contribute to the pressure which at first rises steadily, though at decreasing rate, due to the first diffraction wave from the lower edge. When the corresponding wave from the upper edge arrives, however, the pressure suddenly starts to decrease and reaches a minimum value of about the same magnitude and at about the same time as the corresponding minima for the points P and Q. Beyond this time $t = 3{\cdot}0$ (approximately) the solution (90) is valid up to about $t = 3{\cdot}175$ for the point S, and the calculations show the pressure starting to increase again with values between those for the points P and T; these values are not plotted owing to the difficulty of distinguishing the resulting curve from the curves for P and T.

The curve for the point T on the back of the half-plane is, of course, one already considered in figure 4 and shows a steady increase of pressure with time, with a sudden change in slope at time $t = 3{\cdot}0$ to a smaller but still positive slope.

The curves in figure 6 indicate that for all points to the rear away from the screen at distance $R = 2{\cdot}5$ from the centre-line of the slit, the pressure passes through a minimum value which is of about the same magnitude and occurs at about the same time for all such points. In view of the large variation of the initial shape of the curves in figure 6 it is remarkable that they should converge so quickly and subsequently remain so close together; we shall return to this result later when considering the approximation represented by the broken curve in figure 6.

The preceding discussion refers to points at distance $R = 2{\cdot}5$ from the centre-line of the slit. For corresponding points at large distance R, the same general features will hold but the initial portions for points such as P and Q will become concentrated into thin peaks. Thus for a distant point on the plane of symmetry the pressure will have a sharp front as in the external incident pulse but will then drop very rapidly, in a time of order $1/R$, from the value unity to values of order $1/\sqrt{R}$, with a subsequent minimum value given by equation (94) at approximately $t = R + \frac{1}{2}$. For a distant point on the edge of the shadow, the same features will hold save that the initial thin peak will only rise to a value $p = \frac{1}{2}$. For a distant point at an appreciable angle in the shadow there is no initial peak, and the pressure is small of order $1/\sqrt{R}$ throughout the initial stages.

4·53. *'Pressure flux' through slit*

The pressure flux $Q(t)$ per unit length of slit is given exactly for $t \leqslant 2$ by equations (57) and (66), from which values correct to four decimal places have been computed as quoted in table 7. The corresponding asymptotic solution for $Q(t)$ is given by equation (81) which has been evaluated by numerical integration for $t = 0(0{\cdot}5)4$ to give results also quoted in table 7; these values are estimated to be accurate to 0·0004 or better.

The exact and asymptotic solutions are compared graphically in figure 7, where the initial thick line represents the contribution of $\delta(t)$ to the exact solution. Close agreement is hardly to be expected in the initial stages, but figure 7 and table 7 indicate that by time $t = 1$ the asymptotic solution differs only by 3 % from the exact solution, and that thereafter the difference tends to decrease, becoming only 0·4 % by time $t = 2$.

TABLE 7. VALUES OF $Q(t)$ FROM EXACT AND ASYMPTOTIC SOLUTIONS

t	$Q(t)$ 'exact'	$Q(t)$ 'asymptotic'	t	$Q(t)$ 'exact'	$Q(t)$ 'asymptotic'
0	$1+\delta(t)$	π	1·7	0·9152	—
0·5	1	1·1994	1·8	0·9043	—
1·0	1	1·0316	1·9	0·8942	—
1·1	0·9917	—	2·0	0·8847	0·8880
1·2	0·9790	—	2·5	—	0·8471
1·3	0·9655	—	3·0	—	0·8156
1·4	0·9520	—	3·5	—	0·7902
1·5	0·9391	0·9444	4·0	—	0·7692
1·6	0·9268	—			

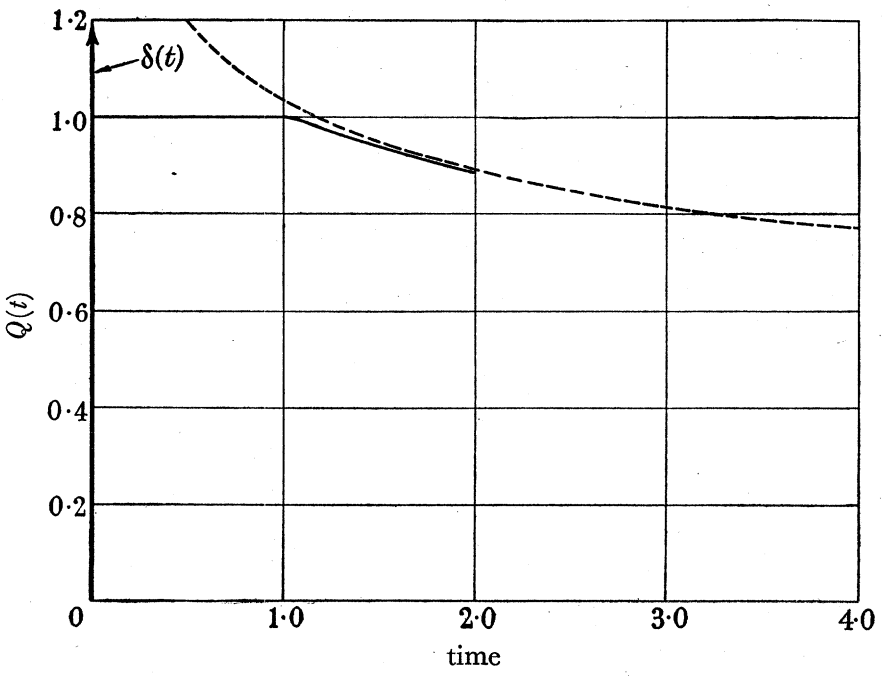

FIGURE 7. Variation of $Q(t)$ with time according to exact (—) and asymptotic (---) solutions.

The preceding comparisons relate to $Q(t)$ which, as defined by equation (52), is the integrated pressure gradient over the width of the slit. It is of interest to examine, therefore, whether the same degree of agreement exists for individual values of the pressure gradient at specific points in the slit. For this purpose we can note first that for incompressible flow, as assumed in the asymptotic solution, the pressure gradient through the slit is given by

$$\psi(y,t) = \frac{Q(t)}{\pi\sqrt{[y(1-y)]}} \tag{96}$$

for any time t. This equation corresponds to a constant shape for the distribution of ψ over the slit, whereas in the pulse problem the distribution of ψ will undoubtedly vary with time. However, for the particular instant $t = 1$, it is easy to show from equations (49) and (50) that ψ is in fact also given in the pulse problem by equation (96) but with $Q(t) = 1$.

Hence at the instant $t = 1$ the percentage agreement between exact and asymptotic solutions is the same for all individual values of ψ as for $Q(t)$, namely, about 3 %. Since thereafter the values for $Q(t)$ in table 7 show a general increase of agreement with increasing

time, it seems reasonable to expect a similar trend for individual values of the pressure gradient ψ in the slit. As a check, calculations have been carried out for time $t = 2$ and are given in table 8. The 'exact' values in this table were obtained by using equations (51) and (50) to determine g_1 by numerical integration, whilst the corresponding values for the asymptotic solution were found from equation (96) with the value $Q(t) = 0{\cdot}8880$ from table 7. In both sets of values in table 8 the errors of calculation are estimated to be at most 0·0004.

TABLE 8. VALUES OF $\psi(y, t)$ WHEN $t=2$

		exact solution	asymptotic solution
$y = 0$,	$\sqrt{y}\,\psi =$	0·2820	0·2827
$y = 0{\cdot}2$,	$\psi =$	0·7040	0·7068
$y = 0{\cdot}4$,	$\psi =$	0·5746	0·5770
$y = 0{\cdot}5$,	$\psi =$	0·5623	0·5654

The comparison in table 8 indicates that at time $t = 2$ the agreement between exact and asymptotic solutions for ψ, whilst varying somewhat from point to point in the slit, is again of the same order as for the corresponding pressure flux $Q(t)$, namely, 0·4 % at this particular instant.

The rapidity with which the pressure gradient in the slit approximates closely to that given by the asymptotic solution based on incompressible flow is not unreasonable physically owing to the nature of the distribution of the gradient over the slit. Thus from the exact solution, for $t>0$ the pressure flux $Q(t)$ is at first completely concentrated at the edges, 50 % at each, and then spreads out over the slit. However, the final asymptotic distribution is also relatively concentrated near the edges, since equation (96) indicates that half of the pressure flux $Q(t)$ is contained in two regions each extending only about one-seventh of the width of the slit from either edge. In effect, therefore, adjustments in distribution of gradient have to take place on average only over distances of a fraction of the width of the slit for which purpose a period $t = 2$, for example, may well be a relatively long time.

4·54. *Pressure distribution near the slit at given times*

Using tables 1 *a* to 3 and the exact solution (44) the pressure on the back of either half-plane has been calculated, to an estimated accuracy of 0·001, for $Y = 0(0{\cdot}2)4$ at times $t = 1, 2, 3, 4$. The results are quoted in table 9 as 'exact' values and plotted as the full curves of figure 8. The pressure distribution on the back of either half-plane thus has an infinite slope at each end and a discontinuity of slope at $Y = t-1$; this latter arises from the finite slope at the front of the second (f_1) diffraction wave.

For comparison, the corresponding incompressible flow distribution has been evaluated to similar accuracy from equation (84), using 'asymptotic' values of $Q(t)$ from table 7, and the results are quoted in table 9 and plotted as the broken curves of figure 8.

Near the pressure front, $Y = t$, the two sets of curves exhibit considerable disagreement, but conversely, near the slit, there is extremely close agreement and the full and broken curves effectively coincide.

Calculations of the exact pressure distribution have also been carried out for points on the plane of symmetry for times $t = 1, 2, 3$ over the relevant ranges of X for which the solution (91) is valid. The results are shown as the full curves in figure 9 and the values

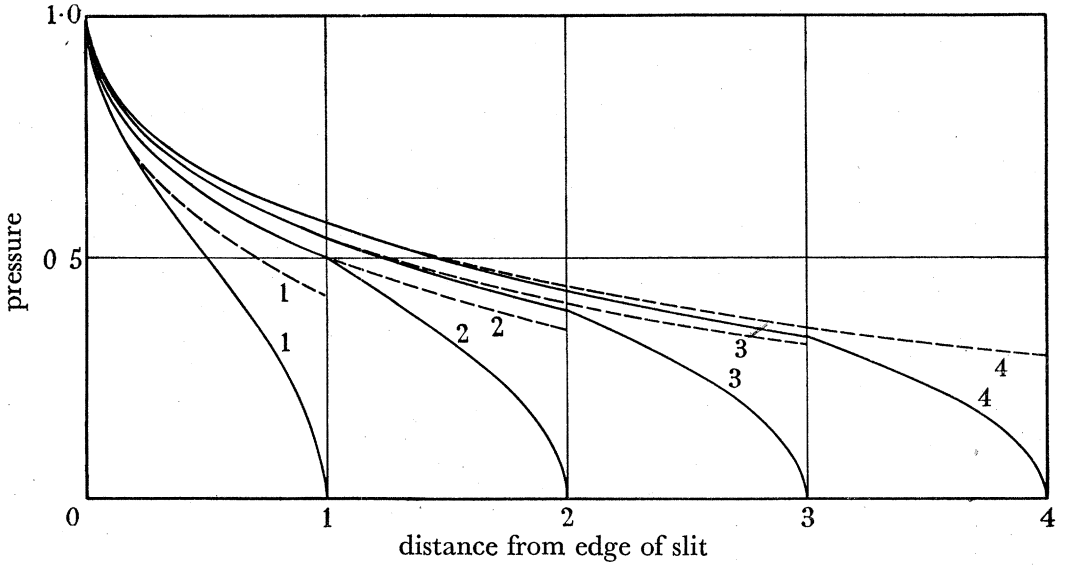

FIGURE 8. Pressure distribution on back of either half-plane at times $t = 1, 2, 3, 4$. — exact; --- incompressible flow.

TABLE 9. COMPARISON OF EXACT AND ASYMPTOTIC SOLUTIONS FOR PRESSURE ON BACK OF HALF-PLANE

	$t=1$		$t=2$		$t=3$		$t=4$	
Y	'exact'	'asymptotic'	'exact'	'asymptotic'	'exact'	'asymptotic'	'exact'	'asymptotic'
0	1	1	1	1	1	1	1	1
0·2	0·705	0·715	0·755	0·755	0·775	0·775	0·788	0·788
0·4	0·564	0·608	0·663	0·663	0·691	0·690	0·708	0·708
0·6	0·436	0·532	0·597	0·597	0·629	0·630	0·651	0·651
0·8	0·295	0·471	0·544	0·545	0·580	0·582	0·605	0·606
1·0	0	0·421	0·5	0·502	0·539	0·542	0·567	0·568
1·2	—	—	0·436	0·464	0·503	0·508	0·534	0·536
1·4	—	—	0·369	0·432	0·471	0·478	0·504	0·508
1·6	—	—	0·295	0·402	0·442	0·451	0·477	0·483
1·8	—	—	0·205	0·377	0·415	0·427	0·452	0·460
2·0	—	—	0	0·352	0·392	0·405	0·430	0·439
2·2	—	—	—	—	0·346	0·384	0·408	0·420
2·4	—	—	—	—	0·295	0·366	0·388	0·402
2·6	—	—	—	—	0·238	0·348	0·369	0·385
2·8	—	—	—	—	0·166	0·332	0·350	0·370
3·0	—	—	—	—	0	0·316	0·333	0·355
3·2	—	—	—	—	—	—	0·295	0·341
3·4	—	—	—	—	—	—	0·253	0·329
3·6	—	—	—	—	—	—	0·205	0·316
3·8	—	—	—	—	—	—	0·144	0·304
4·0	—	—	—	—	—	—	0	0·293

TABLE 10. COMPARISON OF EXACT AND ASYMPTOTIC SOLUTIONS FOR PRESSURE DISTRIBUTION ON PLANE OF SYMMETRY

	$t=1$			$t=2$			$t=3$	
X	'exact'	'asymptotic'	X	'exact'	'asymptotic'	X	'exact'	'asymptotic'
0	1	1	0·866	0·6257	0·6277	1·936	0·4544	0·4643
0·1	0·9367	0·9347	1·0	0·5880	0·5919	2·0	0·4449	0·4562
0·2	0·8768	0·8719	1·2	0·5399	0·5450	2·2	0·4176	0·4322
0·4	0·7746	0·7594	1·4	0·5022	0·5044	2·4	0·3958	0·4101
0·6	0·7109	0·6663	1·6	0·4817	0·4686	2·6	0·3857	0·3897
0·8	0·7563	0·5898	1·8	0·5162	0·4366	2·8	0·4168	0·3707
0·866	1	0·5675	1·936	1	0·4164	2·958	1	0·3517
1·0	1	0·5259	2	1	0·4078	3	1	0·3501

PHILOSOPHICAL TRANSACTIONS OF THE ROYAL SOCIETY A MATHEMATICAL, PHYSICAL & ENGINEERING SCIENCES

labelled 'exact' in table 10. The corresponding incompressible flow distributions have been evaluated from equation (85) using the relevant 'asymptotic' values of $Q(t)$ from table 7. These results are plotted as the broken curves in figure 9 and compared numerically with the exact solution in table 10, where both sets of values are accurate to about 0·0003 or better.

Although the comparisons of figure 9 and table 10 are less extensive than those of figure 8 and table 9, the same type of agreement is apparent, namely, poor agreement near the pressure front changing fairly rapidly to good agreement with decreasing distance from the slit.

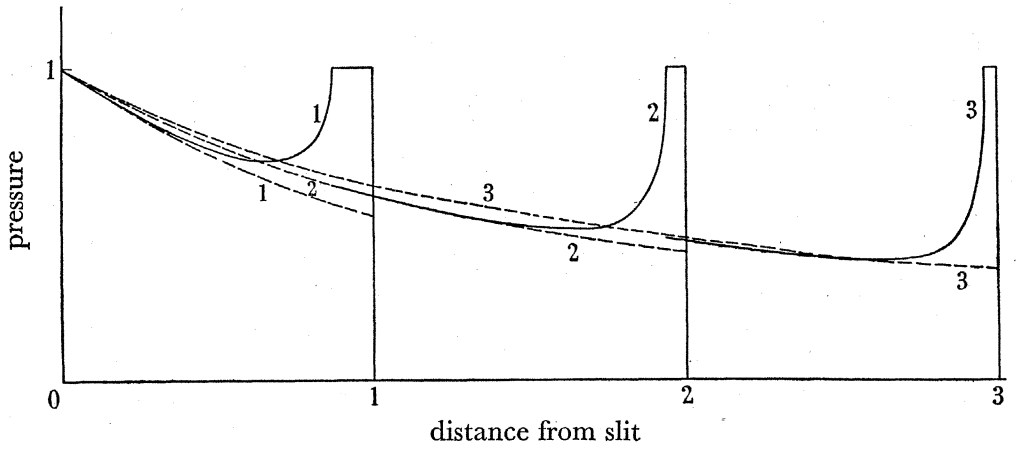

FIGURE 9. Pressure distribution at the rear on the plane of symmetry at times $t = 1, 2, 3$. — exact; --- incompressible flow.

Figures 8 and 9 illustrate clearly the validity of the assumption of § 4·3, that the flow through the slit becomes effectively incompressible within a central region of steadily increasing size.

The preceding comparisons refer to the two cases of points on the screen and points on the plane of symmetry. These may be considered as the two extreme cases, since figure 6 has already indicated that for intermediate angular positions, such as Q and S in figure 6*a*, the phenomena are simply of intermediate character. It seems reasonable therefore to conclude, in particular, from tables 9 and 10 that for all points within a distance of about $R = 2{\cdot}5$ from the centre-line of the slit, the asymptotic solution (82) becomes valid to order 3 % or less by the time of arrival of the second (f_1) diffraction wave from the nearer edge. Within this region $R < 2{\cdot}5$, therefore, the pressure can be determined by using the exact solutions of § 4·4 as long as they are valid and thereafter, to an accuracy of 3 % or better, the solution (82) with $Q(t)$ given by equation (81). This procedure would be much simpler, in general, than using either the exact wave solution (44) for p_b and then equation I (9) or the exact solution (49) for ψ and then equation I (7).

In view of the preceding discussion, the pressure distribution on the plane of symmetry to the rear can be considered in figure 9 to be given by the full curves continued back to the slit, for $t = 2$ and $t = 3$, by the broken curves. The resulting shape of pressure-distance curves is similar, as we might expect, to the corresponding pressure-time variation at each point as illustrated previously by the curve for the point P in figure 6. Both types of curve show an

initial peak which becomes progressively thinner as the pressure front travels to the rear and both types exhibit a minimum value.

These results may be interpreted physically by considering the phenomena to depend broadly on two main processes of equalization. First, within the direct line of the slit ($0 \leqslant y \leqslant 1$), the external pulse tends to be propagated straight on but steadily loses pressure behind its front by equalization to the shadow regions above and below. Secondly, the excess pressure everywhere in front of the screen produces a flow through the slit tending to equalize pressure on both sides of the screen. For a point on the plane of symmetry at some distance to the rear, the first process comes quickly into effective action and produces a decreasing pressure behind the front. The second process, which tends to increase the pressure, is slower in becoming appreciable but ultimately dominates and the pressure increases again. For a point well in the shadow, such as S in figure 6*a*, both processes act together to produce an overall steady increase of pressure subject only to temporary decreases due to 'over-shooting' of the first equalization process.

4·55. *Behaviour of the slit as a source*

The comparisons illustrated in figures 8 and 9 both show that the region of sensibly incompressible flow spreads out from the slit more slowly than the pressure front. Thus, in table 9, if we consider points $Y = t-1$ at unit distance behind the pressure front we find that at $t = 2$ the asymptotic solution is correct to about $\frac{1}{2}$ %, whereas at $t = 4$ it is only accurate to about 7 %. For distant points to the rear for which R is large there will thus be a long period of time after the arrival of the pressure front in which the asymptotic solution is not valid. Further, in the later stages of this period many diffraction waves will be involved, and the exact wave solution will become unmanageable for calculation purposes. However, the approximation (86), regarding the slit as a central source, is expected to be especially suitable for distant points and to become valid earlier than the asymptotic solution (73). Equation (86) will be referred to as the 'source' approximation, and we will now consider some evidence regarding its potential accuracy.

We have already noted in § 4·3 that the 'source' approximation should be especially good for points on the plane of symmetry as indicated for very distant points by the equivalence of equations (88) and (93) for all $t-X$ not small. Conversely, we should also expect, from the assumptions involved, that the 'source' approximation is least accurate in general for points on the half-planes.

As a first numerical comparison we consider the limiting case of distant points on the back of a half-plane for which we can use the exact solution (45) and the special form (87) of the 'source' approximation with $R = Y+\frac{1}{2}$. The results of calculation are shown in table 11, where it must be noted that for the approximate solution the exact form of $Q(t)$ given by (57) and (66) was used with numerical integration of equation (87) for $\mu > 1$. Both sets of values in table 11 are estimated to be accurate to 0·002 or better.

Table 11 shows that for times $t > Y+1 = R+\frac{1}{2}$, the 'source' approximation is in good agreement to about 1 % or less with the exact solution. For corresponding distant points on the plane of the symmetry, as already noted, the agreement will be virtually exact by time $t-R = t-X > \frac{1}{2}$. It seems reasonable to conclude, therefore, that for all distant points, the slit behaves effectively as a central two-dimensional source to an accuracy of order 1 %

TABLE 11. COMPARISON OF EXACT SOLUTION AND 'SOURCE' APPROXIMATION FOR p_b WHEN $Y \to \infty$

$t-Y$	$\sqrt{Y}\,p_b$ 'exact'	$\sqrt{Y}\,p_b$ 'source'	$t-Y$	$\sqrt{Y}\,p_b$ 'exact'	$\sqrt{Y}\,p_b$ 'source'
0·5	0·450	∞	1·2	0·653	0·646
0·6	0·493	0·854	1·4	0·671	0·665
0·7	0·533	0·705	1·6	0·688	0·686
0·8	0·569	0·658	1·8	0·705	0·705
0·9	0·604	0·641	2·0	0·721	0·723
1·0	0·637	0·637			

or less by time $t = R+\frac{1}{2}$. This time, it may be noted, occurs on or before the arrival of the second diffraction wave from the nearer edge.

As a second numerical comparison we can return to the curves given in figure 6 for points at distance $R = 2{\cdot}5$ from the centre-line of the slit. Beyond $t = 3$ all the curves for the different points lie close together, and for comparison the 'source' approximation has been evaluated from equation (86) using the exact forms (57) and (66) for $Q(t)$. The results are indicated by the broken curve in figure 6 which for $t > 2{\cdot}8$ becomes virtually coincident with the curve for point P. Correspondingly, the 'source' approximation is worst for the point T on the half-plane, but even at this point the differences for $t > 3$ are only of order 2 % or less as shown in table 12, where relevant values are quoted to an estimated accuracy of 0·001.

TABLE 12. COMPARISON OF EXACT SOLUTION AND 'SOURCE' APPROXIMATION FOR p_b AT $Y = 2$

t	p_b 'exact'	p_b 'source'	t	p_b 'exact'	p_b 'source'
2·5	0·295	∞	3·1	0·396	0·390
2·6	0·319	0·535	3·2	0·399	0·392
2·7	0·341	0·439	3·4	0·408	0·401
2·8	0·359	0·407	3·6	0·415	0·411
2·9	0·376	0·394	3·8	0·423	0·420
3·0	0·392	0·390	4·0	0·430	0·428

TABLE 13. COMPARISON OF EXACT SOLUTION AND 'SOURCE' APPROXIMATION FOR p_b AT TIME $t = Y+1 = R+\frac{1}{2}$

Y	p_b 'exact'	p_b 'source'	Y	p_b 'exact'	p_b 'source'
0	1	0·787	1·8	0·408	0·406
0·2	0·732	0·687	2·0	0·392	0·390
0·4	0·641	0·619	2·2	0·378	0·376
0·6	0·581	0·567	2·4	0·365	0·364
0·8	0·536	0·527	2·6	0·353	0·352
1·0	0·5	0·494	2·8	0·343	0·342
1·2	0·471	0·466	3·0	0·333	0·333
1·4	0·447	0·443	4·0	0·295	0·295
1·6	0·426	0·423	6·0	0·247	0·247

In both the preceding comparisons, good agreement commences at about $t = R+\frac{1}{2}$. At this time, by use of equation (57), the 'source' approximation (86) gives

$$p \sim \frac{1}{\pi\sqrt{(Y+0{\cdot}75)}} + \frac{1}{\pi}\cosh^{-1}\left(\frac{2Y+2}{2Y+1}\right) \quad (t = Y+1 = R+\tfrac{1}{2}), \tag{97}$$

for a point on the back of either half-plane whilst the corresponding exact solution (44) gives

$$p = \frac{2}{\pi}\tan^{-1}\left(\frac{1}{\sqrt{Y}}\right) \quad (t = Y+1). \tag{98}$$

Equations (97) and (98) have been evaluated to give the comparison shown in table 13, which shows an overall trend for increasing agreement with increasing distance from the slit.

Generally, for large $R\to\infty$, the 'source' approximation (87) gives by use of (57)

$$p \sim \frac{2}{\pi\sqrt{R}} \quad (R\to\infty,\ t = R+\tfrac{1}{2}), \tag{99}$$

for any point to the rear at distance R from the centre line of the slit. This equation (99) agrees with the exact limiting form (94) for a point in the plane of symmetry and with the limiting form of the exact solution (98) for a point on the back of either half-plane; similarly, it can be shown from equation (90) that the same limiting form holds for any point in the shadow of large X and Y. Hence for any distant point to the rear the source approximation agrees with the exact solution at time $t = R+\frac{1}{2}$ in the limit $R\to\infty$.

4·56. *Approximate procedure for determining pressure*

The preceding comparisons indicate that for $R>2{\cdot}5$ the agreement between the 'source' approximation, and the exact solution becomes especially good at time $t = R+\frac{1}{2}$ and that thereafter the difference will be oscillatory in magnitude, of order 2 % or less, and presumably decaying with increasing time. It would thus appear that to an accuracy of order 2 % or less, the 'source' approximation can be used to obtain the pressure for all points $R>2{\cdot}5$ at all times after the exact solutions of § 4·4 cease to be valid. This region $R>2{\cdot}5$ is complementary to the region $R<2{\cdot}5$ within which it was previously concluded that the asymptotic solution could similarly be used. Thus, to an accuracy of order 3 % or less, the pressure in our particular problem can be determined everywhere to the rear of the screen by using (*a*) the relatively simple exact solutions of § 4·4 so long as they are valid, and thereafter either the asymptotic solution or the 'source' approximation. For the inner region $R<2{\cdot}5$ the former only would be used, but for more distant points the source approximation would be used first and later replaced by the simpler asymptotic solution which ultimately becomes accurate for any point, however distant.

Both the asymptotic solution and the 'source' approximation depend primarily on a knowledge only of $Q(t)$ which is given exactly by equations (57) and (66) for $t\leqslant 2$ and thereafter to good accuracy by equation (81).

Such use of the approximate expressions (82) and (86), or their special forms (73), (84), (85) and (87) where relevant, gives a practical alternative to the relatively laborious calculations necessary in the formal exact wave solution when many waves are involved, especially if a point not on a half-plane is under consideration and equation I (7) or I (9) must be used for the exact solution. When using the approximate method we can, of course, still use the simple equation I (1) to determine pressures in front of the screen from a knowledge of the pressure at image points to the rear.

5. Conclusion

In the present paper a general method has been indicated by which the results of a previous paper (Fox 1948) could be used without *formal* difficulty to derive an explicit solution for any two-dimensional pulse problem involving strips or half-planes as obstacles. The method has been used to obtain the general form of solution for an infinite slit in a perfectly reflecting screen subjected to any known incident two-dimensional pulse field (figure 2).

Numerical results have been obtained for the particular case of a plane $H(t)$ pulse (figure 3) incident normally on such a screen. The most interesting pressure phenomena are those occurring initially in the direct line of the slit as illustrated in figures 6 and 9. Apart from these initial phenomena the general process of ultimate equalization of pressure through the slit appears to be, in general, of a steady asymptotic character. In particular, there is no evidence for the pressure to the rear ever exceeding the ultimate value of unity, and conversely, by equation I (1), the pressure in front would similarly never drop below unity after the arrival of the pulse. In this respect the slit problem differs from the corresponding strip problem of paper I in which the ultimate pressure equalization appears to be essentially a decaying oscillatory process.

Possibly the most interesting result of the calculations is the rapidity with which the flow through the slit becomes effectively incompressible and the corresponding early validity of the asymptotic solution in a region near the slit. Similarly, for more distant points it is interesting to find that the slit behaves as a central source to fair accuracy relatively soon after the arrival of the initial diffraction wave.

The related problem of a regular grating subjected to a plane pulse at normal incidence can be solved without difficulty by using the method of § 2, and results which have been obtained for this problem will be considered in a further paper.

References

Carslaw, H. S. & Jaeger, J. C. 1941 *Operational methods in applied mathematics*. Oxford: University Press.
Fox, E. N. 1948 *Phil. Trans.* A, **241**, 71.
Friedlander, F. G. 1946 *Proc. Roy. Soc.* A, **186**, 322.
Jeans, J. H. 1925 *Mathematical theory of electricity and magnetism*, 4th ed. Cambridge: University Press.
Lamb, H. 1932 *Hydrodynamics*, 6th ed. Cambridge: University Press.
Whittaker, E. T. & Watson, G. N. 1927 *Modern analysis*, 4th ed. Cambridge: University Press.

PHILOSOPHICAL TRANSACTIONS OF THE ROYAL SOCIETY A MATHEMATICAL, PHYSICAL & ENGINEERING SCIENCES